Bayesian analysis of signal deconvolution using measured instrument response functions

Pascal Pernot

Bayesian analysis of signal deconvolution using measured instrument response functions

Pascal PERNOT
Laboratoire de Chimie Physique, (UMR 8000, associated to CNRS)
Bât. 349, Université Paris-Sud, 91405 Orsay Cedex, France
email: pascal.pernot@lcp.u-psud.fr

April 14, 2006

Abstract

Using measured instrumental response functions for data deconvolution is a known source of uncertainty. This problem is revisited here with Bayesian data analysis an Monte Carlo simulations. Noise correlation induced by the convolution operator is identified as a major source of uncertainty which has been neglected in previous treatments of this problem. Application to a luminescence lifetime measurement setup shows that existing approximate treatments are markedly defficient and that the correlation length of the noise is directly related to the lifetime to be estimated. Simple counteractive treatments are proposed to increase the accuracy of this procedure.

1 Introduction

The deconvolution problem is a classical inverse problem, and has received a lot of attention in many scientific and engineering fields. The instrument response function (IRF), also called blurring function, is generally assumed to be accurately determined. It is however not uncommon that the IRF is measured with the same accuracy as the signal to be treated, due to instrumental or experimental design constraints. The impact of an uncertain IRF on the accuracy of the deconvolved signal has to be considered with care. This uncertainty propagation issue has been addressed in the past by Dose *et al.* [1]. We show here analytically and numerically that their approximate solution does not encompass important effects of noise correlation due to convolution.

In this paper, we use Bayesian data analysis to derive an exact expression of the likelihood function in the case of gaussian additive noise. This solution is applied to the classical problem of lifetime estimation from luminescence data.

2 Theory

The observed signal vector $\mathbf{s}$ (length n) is generally expressed as a linear reconvolution model

$$\mathbf{s} = \mathbf{H}\mathbf{m} + \mathbf{e}_s, \tag{1}$$

where $\mathbf{m}$ is a vector of values of the model function at the measurement points, $\mathbf{H}$ is a $n \times n$ zero-padded lower triangular Toeplitz matrix built from the IRF $\mathbf{h}$ of length n_h

$$\mathbf{H} = \begin{pmatrix} h_1 & 0 & \cdots & 0 & 0 \\ h_2 & h_1 & \cdots & 0 & 0 \\ \vdots & \vdots & \ddots & 0 & 0 \\ h_{n_h} & h_{n_h-1} & & h_1 & 0 \\ 0 & h_{n_h} & \cdots & h_2 & h_1 \end{pmatrix} \tag{2}$$

and $\mathbf{e}_s$ is an additive noise with multinormal statistics and covariance matrix $\mathbf{R}_s$:

$$\mathbf{e}_s \sim \mathcal{N}_n(0, \mathbf{R}_s). \tag{3}$$

Note that we use bold lowercase symbols for vectors ($\mathbf{s}$) and bold capitals for matrices ($\mathbf{H}$).

Using the symmetry property of convolution, Eq. 1 can also be written

$$\mathbf{s} = \mathbf{M}\mathbf{h} + \mathbf{e}_s \tag{4}$$

where $\mathbf{M}$ is a $n \times n_h$ lower triangular Toeplitz matrix built from the model vector $\mathbf{m}$ as shown above (Eq. 2).

As the exact IRF is generally not known, a measured IRF is used instead to solve Eq.1 or Eq.4. A multinormal additive noise model is also used for the IRF

$$\mathbf{h} = \hat{\mathbf{h}} + \mathbf{e}_h, \tag{5}$$

where $\hat{\mathbf{h}}$ is the unknown exact IRF and $\mathbf{e}_h \sim \mathcal{N}_{n_h}(0, \mathbf{R}_h)$.

The problem is to reconstruct the model vector $\mathbf{m}$, knowing $\mathbf{s}$, $\mathbf{R}_s$, $\mathbf{h}$ and $\mathbf{R}_h$, and to evaluate the impact of the measurement uncertainties of $\mathbf{h}$ on $\mathbf{m}$. This is an inverse problem doubled with an uncertainty propagation problem. Bayesian data analysis is very well suited to handle this kind of problem **(author?)** [2, 6, 5, 3].

2.1 Bayesian data analysis

The posterior probability density function (pdf) for $\mathbf{m}$ is obtained by Bayes's formula

$$p(\mathbf{m}|\mathbf{s}, \mathbf{R}_s, \mathbf{h}, \mathbf{R}_h) = \frac{p(\mathbf{m})}{p(\mathbf{s})} p(\mathbf{s}|\mathbf{m}, \mathbf{R}_s, \mathbf{h}, \mathbf{R}_h), \tag{6}$$

where $p(\mathbf{m})$ and $p(\mathbf{s})$ are the prior pdf's for $\mathbf{m}$ and $\mathbf{s}$, and where $p(\mathbf{s}|\mathbf{m}, \mathbf{R}_s, \mathbf{h}, \mathbf{R}_h)$ is the likelihood function. Given our model, we do not know explicitely this latter function. Instead, we know the

explicit expression for the likelihood when the exact IRF $\hat{\mathbf{h}}$ is considered (cf. Eq. 3)

$$p(\mathbf{s}|\mathbf{m}, \mathbf{R}_s, \hat{\mathbf{h}}) \sim \mathcal{N}_n(\mathbf{M}\hat{\mathbf{h}}, \mathbf{R}_s). \tag{7}$$

Applying the marginalization rule and knowing the expression of the pdf for $\hat{\mathbf{h}}$

$$p(\hat{\mathbf{h}}|\mathbf{h}, \mathbf{R}_h) \sim \mathcal{N}_n(\mathbf{h}, \mathbf{R}_h), \tag{8}$$

we can write

$$p(\mathbf{m}|\mathbf{s}, \mathbf{R}_s, \mathbf{h}, \mathbf{R}_h) = \frac{p(\mathbf{m})}{p(\mathbf{s})} \int d\hat{\mathbf{h}}\, p(\mathbf{s}|\mathbf{m}, \mathbf{R}_s, \hat{\mathbf{h}}) p(\hat{\mathbf{h}}|\mathbf{h}, \mathbf{R}_h). \tag{9}$$

Considering that in our model $p(\mathbf{s})$ is a normalization constant, and expliciting the pdf's, one gets

$$p(\mathbf{m}|\mathbf{s}, \mathbf{R}_s, \mathbf{h}, \mathbf{R}_h) \propto p(\mathbf{m}) \int d\hat{\mathbf{h}}\ \exp\left(-\frac{1}{2}J\right), \tag{10}$$

where

$$\begin{aligned} J &= (\mathbf{s} - \mathbf{M}\hat{\mathbf{h}})^T \mathbf{R}_s^{-1} (\mathbf{s} - \mathbf{M}\hat{\mathbf{h}}) \\ &+ (\mathbf{h} - \hat{\mathbf{h}})^T \mathbf{R}_h^{-1} (\mathbf{h} - \hat{\mathbf{h}}). \end{aligned} \tag{11}$$

This quantity is rearranged in order to enable analytical integration

$$\begin{aligned} J &= (\hat{\mathbf{h}} - \mathbf{h}_0)^T \mathbf{P}^{-1} (\hat{\mathbf{h}} - \mathbf{h}_0) - \mathbf{h}_0^T \mathbf{P}^{-1} \mathbf{h}_0 \\ &+ \mathbf{s}^T \mathbf{R}_s^{-1} \mathbf{s} + \mathbf{h}^T \mathbf{R}_h^{-1} \mathbf{h}, \end{aligned} \tag{12}$$

where

$$\begin{cases} \mathbf{P} &= \left(\mathbf{M}^T \mathbf{R}_s^{-1} \mathbf{M} + \mathbf{R}_h^{-1}\right)^{-1} \\ \mathbf{h}_0 &= \mathbf{P}(\mathbf{M}^T \mathbf{R}_s^{-1} \mathbf{s} + \mathbf{R}_h^{-1} \mathbf{h}) \\ &= \mathbf{h} + \mathbf{P}\mathbf{M}^T \mathbf{R}_s^{-1} (\mathbf{s} - \mathbf{M}\mathbf{h}) \end{cases} \tag{13}$$

Integration over $\hat{\mathbf{h}}$ finally leads to

$$p(\mathbf{m}|\mathbf{s},\mathbf{R}_s,\mathbf{h},\mathbf{R}_h) \propto \frac{p(\mathbf{m})}{|\mathbf{P}|^{1/2}} \exp\left(-\frac{1}{2}(\mathbf{s}-\mathbf{M}\mathbf{h})^T\mathbf{K}(\mathbf{s}-\mathbf{M}\mathbf{h})\right), \tag{14}$$

where

$$\mathbf{K} = \mathbf{R}_s^{-1} - \mathbf{R}_s^{-1}\mathbf{M}\mathbf{P}\mathbf{M}^T\mathbf{R}_s^{-1}. \tag{15}$$

This expression for the posterior pdf calls for a few comments :

- convolution of the model vector with a noisy IRF leads to a "noisy model" $\tilde{\mathbf{m}} = \mathbf{M}\mathbf{h}$, affected by correlated noise with covariance matrix $\mathbf{K}^{-1}$, the structure of which depends explicitely on the model vector itself (heteroscedastic correlated noise). This is in contrast with the result of Dose *et al.* **(author?)** *[1]*, who obtain an expression for an effective variance, and do not consider the covariance part.

- the mode of the posterior pdf depends on the actual value of the measured IRF $\mathbf{h}$. A bias in the optimal values for the model vector is thus to be expected, as a different realization of the IRF would lead to a different solution. In any case, a consistent uncertainty analysis should ensure that the exact value lies within confidence intervals.

3 Application

An application of interest is for instance the lifetime estimation of unstable chemical species from their luminescence decays.

3.1 Model

A mono-exponential decay signal with lifetime τ is generated over a regular time grid ($n_h = n = 100$). The model is $m_i = \exp(-t_i/\tau)$. The IRF is a gaussian function centered at t_0, and of FWHM w_h

$$h_i = \exp\left(-4\ln(2)(t_i - t_0)^2/w_h^2\right). \tag{16}$$

In order to keep a single parameters, the model after convolution is rescaled to the maximal value of the signal, and we can set $p(\tau|\mathbf{s}, \mathbf{R}_s, \mathbf{h}, \mathbf{R}_h) \equiv p(\mathbf{m}|\mathbf{s}, \mathbf{R}_s, \mathbf{h}, \mathbf{R}_h)$. Homoscedastic noise is considered for both signal and IRF, i.e. $\mathbf{R}_s = \sigma_s^2 * \mathbf{I}_n$, $\mathbf{R}_h = \sigma_h^2 * \mathbf{I}_{n_h}$. Finally, a uniform prior distribution for τ is used ($p(\tau) = cte$).

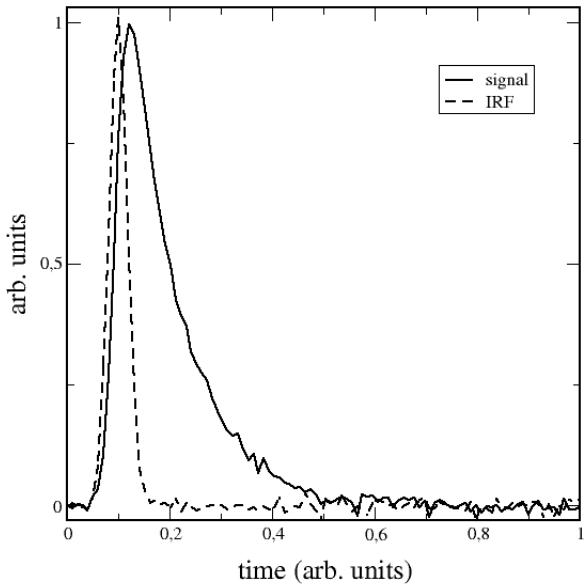

Figure 1: Typical synthetic signal and IRF used for lifetime estimation ($\sigma_s = \sigma_h = 0.01$, $\tau = 0.1$ $t_0 = 0.1$and $w_h = 0.03$).

3.2 Comparison of models of the posterior pdf

The exact expression for the posterior pdf (eq.15) is compared to approximate expressions :

- no correction for the noisy IRF ($\sigma_h = 0$, in our model), which is the most commonly used method;
- the diagonal approximation of eq.15, which implements some level of variance correction, but fails to encompass the correlation in the model's noise;
- the "effective variance" method [1, 7].

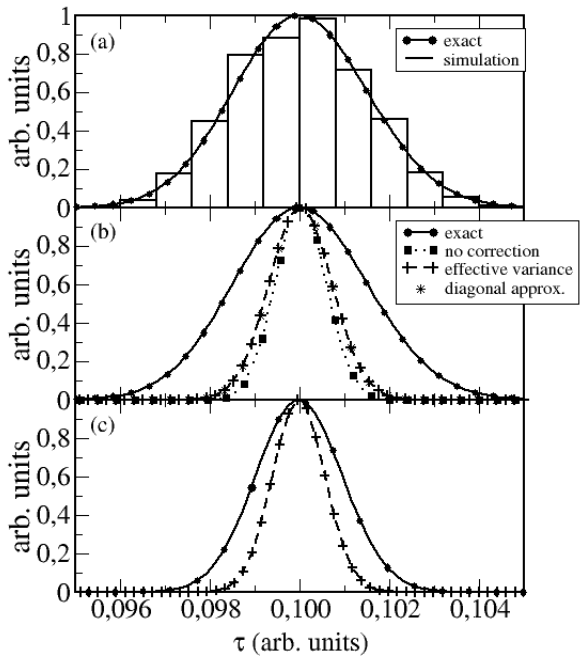

Figure 2: Posterior density functions for the lifetime estimated from a noisy decay and for different treatments of the IRF's uncertainty ($\sigma_h = \sigma_s = 0.01$). The functions have been shifted and renormalized to facilitate direct comparison. (a) comparison of simulation results (1000 runs) with the full bayesian solution proposed in the present work; (b) comparison of the full treatment with various approximations (see text), full support of the IRF; (c) support of the IRF limited to $t \leq 0.2$ (all approximate methods are undiscernable).

Variance. Fig. 2 represents the posterior pdf $p(\tau|\mathbf{s}, \sigma_s, \mathbf{h}, \sigma_h)$ computed by Monte Carlo simulation, and by the different methods in the case of a same measurement accuracy for the signal and the IRF ($\sigma_h = \sigma_s = 0.01$). The Monte Carlo method consists in repeated analysis of randomly noised signal and IRF to build histograms of the maximum a posteriori (MAP) lifetime values (modes of the posterior pdf). All curves have been shifted to a common mode, in order to facilitate comparison. The exact expression is fully coherent with the histogram resulting of the simulation, i.e. it takes properly the variance of the signal and the variance of the IRF into account. It can be seen on this figure that the approximate methods all perform quite similarly and fail to recover the full variance of the lifetime. The "effective variance" method is seen to be numerically equivalent to the diagonal approximation

of our method, and it performs only slightly better than the totally uncorrected method. Correlation in the noise of the convolved model can thus have a major impact on uncertainty quantification.

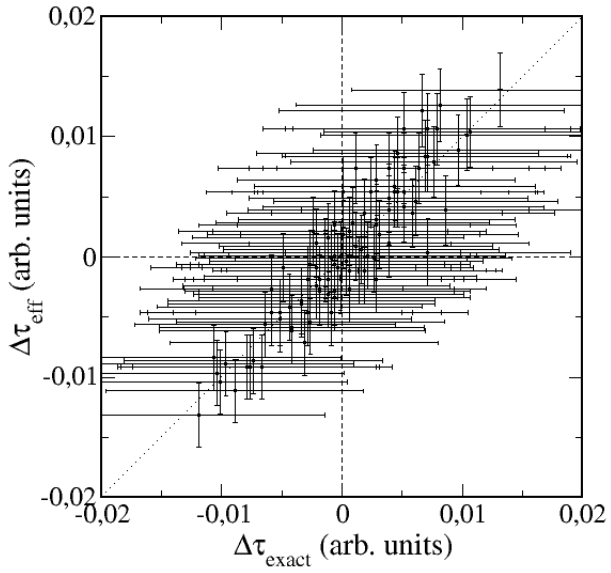

Figure 3: Error estimates and 95% confidence intervals for the lifetime recovered simultaneously by the exact method $\Delta\tau_{exact}$ and by the effective variance method $\Delta\tau_{eff}$ for 100 randomly noised signals and IRF's ($\sigma_h = \sigma_s = 0.01$).

Bias. All methods perform similarly with regard to the bias on lifetime estimation (Fig. 3). In this figure, we reported the estimation by the "effective variance" method as function of the estimation by the exact method. The biases of both methods are highly correlated and practically identical. However, underestimation of the confidence intervals by the approximate method results in inconsistent estimations, i.e. it fails significantly more than the exact method to include the exact value inside the confidence interval, and confidence intervals for different realizations of the noise are frequently disjoint. In this regard, Eq. 15 performs much better.

Accuracy of the IRF. For a given lifetime, when the IRF is measured with a better accuracy ($\sigma_h < \sigma_s$), the differences observed between the various methods tend to vanish (Fig.4). For instance, if the IRF is ten times more accurate than the signal, the uncorrected method provides exact results over all the practical range of lifetimes. It is also observed that longer lifetimes are relatively more affected than shorter ones, which is a pure effect of noise correlation (see next section).

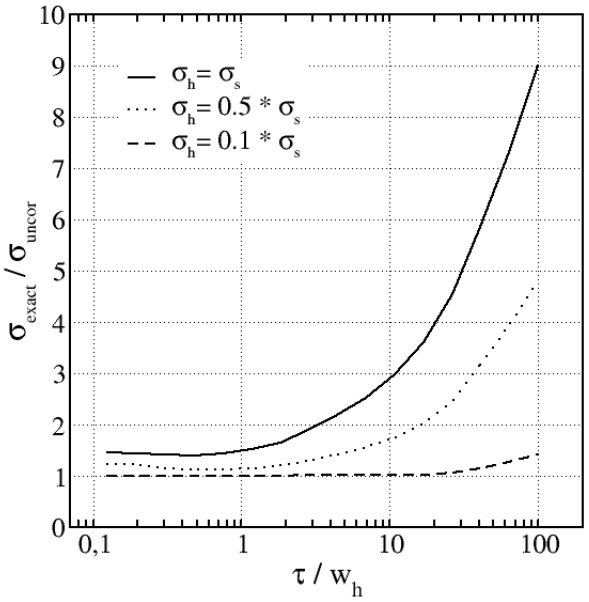

Figure 4: Ratio of the standard deviations of the posterior pdf for the exact model (σ_{exact}) and for the uncorrected model (σ_{uncor}) as a function of the theoretical lifetime.

3.3 Structure of the correlation matrix

The convolution of the mono-exponential model by the IRF is a vector $\tilde{\mathbf{m}}$ which elements obbey the following reccurence

$$\tilde{\mathbf{m}}_i = \exp(-\frac{\Delta t}{\tau})\tilde{\mathbf{m}}_{i-1} + \hat{\mathbf{h}}_i + \mathbf{e}_{h,i}. \tag{17}$$

As soon as the IRF vanishes the correlation between consecutive points is

$$< \tilde{\mathbf{m}}_i, \tilde{\mathbf{m}}_{i-1} >= \exp(-\frac{\Delta t}{\tau}) \tag{18}$$

As there is supposedly no correlation in the signal noise, the covariance matrix $\mathbf{K}$ preserves this correlation scheme. An approximation of the correlation matrix can thus been expressed as

$$\mathbf{C} = \begin{pmatrix} 1 & \rho & \rho^2 & \cdots & \rho^n \\ \rho & 1 & \rho & \cdots & \rho^{n-1} \\ \vdots & \vdots & \ddots & \cdots & \vdots \\ \vdots & \vdots & \vdots & 1 & \rho \\ \rho^n & \rho^{n-1} & \cdots & \rho & 1 \end{pmatrix}, \tag{19}$$

where $\rho = \exp(-\frac{\Delta t}{\tau})$. The noise correlation decays thus exponentially with de delay between points of the model, the decay rate being the inverse of the theoretical lifetime.

3.4 Support length of the IRF

When the IRF is recorded on the same support as the signal, most of the its elements are pure noise. We saw above that these points contribute significantly to the correlation of the noise in the convolved model. Limiting the support of the IRF ($n_h < n$), or zeroing it's purely noisy elements might thus enable to improve the correlation matrix. If we observe the standard deviation for the convolved model (Fig. 5), we see that the truncation of the support of the IRF contributes significantly to reduce the uncertainty at larger times. As shown on Fig.2(c), this enables some uncertainty reduction for the lifetime estimation, but the effect of the correlated noise is still quite marked.

3.4.1 Identifiability

The behaviour of the present model with regard to the limits of detection of lifetimes due to the IRF has been tested by reconstructing the posterior pdf from synthetic signals generated with very small lifetimes. The posterior pdf displays explicitely the non identifiability of lifetimes that are too small (Fig. 6). When τ decreases, the pdf becomes asymmetric, defining an upper limit for the lifetime, but no lower limit, except the one imposed by the prior.

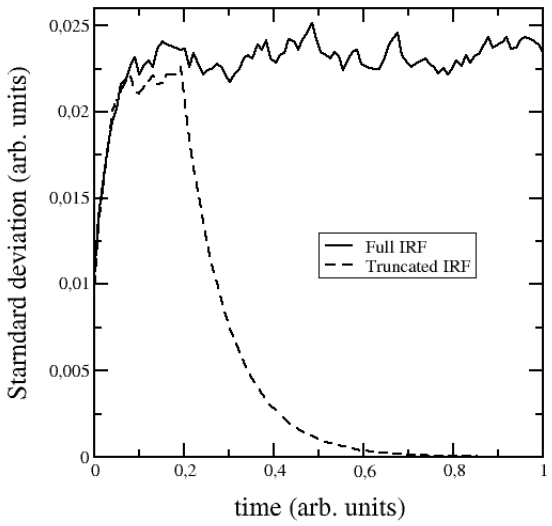

Figure 5: Standard deviation of the model, after convolution with the IRF. Full line : IRF with full support; dashed line : IRF with support limited to $t \leq 0.2$. Same parameters as for Fig. 2.

4 Conclusion

The use of measured instrumental response functions for data deconvolution is a source of uncertainty. We derived a new expression of the likelihood within a bayesian framework to explicitely incorporate this effect and display it's importance. Convolution of a noisy IRF with a model curve produces a noisy model curve with correlated noise.

This has been illustrated on a luminescence lifetime measurement setup, for which it was shown that existing approximate treatments were markedly defficient. It was also shown that, in this case, the correlation length of the noise was directly related to the lifetime to be estimated. Longer lifetimes are thus counterintuitively more affected by IRF's uncertainty that shorter ones. Although the most efficient way to reduce this effect is clearly to improve the IRF's measurement accuracy, we have shown that an qualitative improvement can very simply be obtained by zeroing those parts of the IRF consisting of pure noise.

The method has been applied to an homoscedastic noise pattern, but extension to cases where the noise is dependent on signal intensity (e.g. photon counting methods) is straightforward, as long

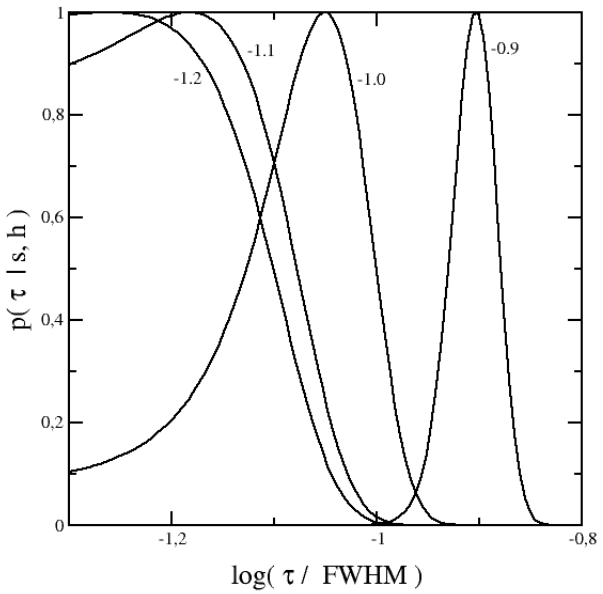

Figure 6: Evolution of the (unnormalized) posterior pdf for τ at the resolution limit of the experimental setup. The exact values for τ are reported alongside the curves. The standard deviation for signal and IRF is $\sigma_s = \sigma_h = 0.005$.

as the normal noise distribution approximation is valid. Similarly, cases where the IRF is locally fluctuating due to minor modifications of the experimental setup can be easily treated by a carefull modelling of the variance/covariance matrix.

We are studying extension of this method to Poisson uncertainties. Evaluation of the resolution limits of a fluorescence TCSCP apparatus [4]. Consistent uncertainty estimation for lifetimes recovered from fluorescence spectra analysis.

An alternative treatment is to modelize the IRF by a function, which parameters pdf's are estimated by a bayesian analysis

$$p(\mathbf{m}|s, \mathbf{R}_s, \mathbf{h}, \mathbf{R}_h) = \frac{p(\mathbf{m})}{p(\mathbf{s})} \int d\mathbf{p}_h \, p(\mathbf{s}|\mathbf{m}, \mathbf{R}_s, \mathbf{p}_h) p(\mathbf{p}_h|\mathbf{h}, \mathbf{R}_h).$$

References

[1] V. Dose, R. Fischer, and W. von der Linden. Deconvolution based on experimentally determined apparatus functions. In G. Erickson, editor, *Maximum Entropy and Bayesian Methods*, pages 147–152. Kluwer Academic, Dordrecht, 1998.

[2] A. Gelman, J. B. Carlin, H. S. Stern, and D. B. Rubin. *Bayesian Data Analysis*. Chapman & Hall, London, 1995.

[3] K. M. Hanson. A framework for assessing uncertainties in simulation predictions. *Physica D*, 133:179–188, 1999.

[4] A. K. Livesey and J. C. Brochon. Analysing the distribution of decay constants in pulse-fluorimetry using the maximum entropy method. *Biophys. J.*, 52:693–706, 1987.

[5] S. J. Press. *Bayesian Statistics: Principles, Models, and Applications*. Wiley, New York, 1989.

[6] D. S. Sivia. *Data Analysis: A Bayesian Tutorial*. Clarendon (Oxford Univ. Press), Oxford, 1996.

[7] U. v Toussaint, R. Fischer, K. Krieger, and V. Dose. Depth profile determination with confidence intervals from rutherford backscattering data. *New Journal pf Physics*, 1:11.1–11.13, 1999.